A Practical Design for a Multivariable Proportional−Integral Controller in Industrial Applications

Daw-Shang Hwang[†] and Pau-Lo Hsu*,[‡]

Institutes of Electronic Engineering and of Control Engineering, National Chiao Tung University, Hsinchu, Taiwan, 300 Republic of China

This paper proposes a robust proportional−integral (PI) controller design for multivariable complex processes to achieve both well-decoupled and well-damped output behavior. By reformulating PI-controlled processes in a way similar to the LQG/LTR control design problem, the proposed model matching technique in the first design stage successfully results in the robust PI controller with well-decoupled output behavior and sufficient stability. Moreover, control performance can be further improved to achieve well-damped responses by applying gain modification in a second design stage. Both simulated results using chemical processes and experimental results using a wind tunnel have proven the feasibility of the proposed PI controller design in real applications.

1. Introduction

The proportional−integral−derivative (PID) controller is the most widely used controller in the process industries because of its simple structure and wide applicability to various processes. Although significant developments in modern control theories have been made recently, over 90% of industrial controllers are still of the PI-type, due to the problems caused by process noise (Deshpande, 1989). Over the years, many well-known formulas have been derived to tune PI (PID) controllers (Åström et al., 1993). However, due to the existence of complex interactions, the extension of the single-loop design procedure for PI(PID)-type controllers to multivariable processes cannot be straightforward unless they are transformed into decoupled systems. Therefore, in addition to the requirement for stability, removing interactions while providing satisfactory control performance is a major concern in designing multivariable PI controllers for complex industrial processes. Generally, methods for obtaining the PI gain matrices can be classified into two categories: on-line tuning and off-line design. In the on-line tuning method, an approximate process model is obtained experimentally and the PI controller adopted is usually incorporated in a multiloop structure (Luyben, 1986; Loh et al., 1993; Friman and Waller, 1994). These approaches usually are required to verify a suitable pairing between inputs and outputs before tuning (Bristol, 1966; Grosdidier and Morari, 1986; Seborg et al., 1989; Hwang, 1995). Usually, each loop is tuned with all other loops open, to adjust performance, and then detuned as they are all put into closed loop to reduce interaction. In this controller structure, a compromise has to be made between performance adjustment and interaction elimination.

On the other hand, if a reasonable process model is available, the off-line design method can be applied. Compared to the multiloop controller, more design freedom for a multivariable controller can be used to adjust control performance and reduce interaction si-

multaneously. In time-domain approaches, PI controller design methods that use the state feedback approach have been reported (Wong and Seborg, 1985; Pulleston and Mantz, 1993). However, direct state feedback may be impractical since states are not usually measurable. Necessary and sufficient conditions for achieving a robust PI controller in the output feedback structure have been discussed by Pohjolainen (1982), Morari (1985), and Lunze (1989). Some PI controllers use simple formula to determine controller gains (Penttinen and Koivo, 1980; Pohjolainen, 1982), with additional fine tuning through a trial-and-error approach. Lewis (1992) formulated a PI-controlled system as a linear quadratic output feedback design problem, but achieving a desirable performance is not straightforward. Eigenstructure assignment was employed for PI controller design (Han, 1989) so that stability can be more easily achievable by assigning stable poles, but numerical complexity in selecting the appropriate eigenstructure is unavoidable. Using frequency domain design, Chen and Munro (1989) proposed a decoupled design via the Nyquist array method, but this involves intensive computation. More intuitively, Knoop and Perez (1993) proposed a model matching approach to design a PI controller without providing a direct approach to choose a suitable reference model and achieve satisfactory robustness. Although many approaches to PI control design have been proposed using various assumptions, engineers and researchers are still pursuing effective methods to achieve satisfactory stability and performance for PI-controlled processes.

In this paper, we will present a robust PI controller design which achieves both well-decoupled and well-damped performance using a straightforward approach based on the frequency response criteria. Basically, robust stability and performance requirements are more conveniently represented in the frequency domain (Safonov et al., 1981; Stein and Athans, 1987; McFarlane and Glover, 1992). Moreover, the linear quadratic gaussian/loop transfer recovery (LQG/LTR) loop shaping design methodology can be appropriately applied to multiinput multioutput (MIMO) processes to achieve a robust observer-based controller (Athans, 1986; Stein and Athans, 1987). We reformulate the PI-controlled loop using a format similar to that employed in LQG/LTR design, so that the strategy used in LQG/LTR loop

---

* Author to whom all correspondence should be addressed. Telephone: 886-3-5712121, ext. 54362. Fax: 886-3-5715998. E-mail: plhsu@cc.nctu.edu.tw.
[†] Institute of Electronic Engineering.
[‡] Institute of Control Engineering.

shaping can be directly employed. The proposed method includes two design stages. A target open-loop model, called the Kalman filter loop, is constructed which renders satisfactory closed-loop stability with well-decoupled time responses. In the first stage, based on a model matching technique, the PI-controlled loop is matched to this target loop by a derived approximation theory. Once a low-interaction design is attained, we can then improve the performance of each channel output individually in the second stage to achieve well-damped output responses, as shown in the second simulation example. This robust PI controller was also tested in the wind tunnel experiments to verify its effectiveness and feasibility.

2. Formulation

Consider a linear dynamic process represented by a general state-space equation as in the following:

$$\dot{x}_p = \mathbf{A}x_p + \mathbf{B}u$$

$$y = \mathbf{C}x_p \tag{1}$$

where x_p, u, and y are state, control, and output, respectively, and the matrices $\mathbf{A}$, $\mathbf{B}$, and $\mathbf{C}$ are of appropriate dimensions. Note that, if the available process model is in a transfer function description, it can be directly represented in a state-space model as in eq 1 (as shown in Example 1, section 5). For most PI-controlled processes, the number of inputs and outputs is assumed to be the same without loss of generality; the PI controller can then be represented as

$$\dot{x}_c = K_i(r - y)$$

$$u = x_c + K_p(r - y) \tag{2}$$

where x_c is the controller state, r is the setpoint, and K_p and K_i are the proportional and integral gain matrices, respectively. Furthermore, if we combine the dynamic process in eq 1 and the PI controller in eq 2 with the concern of measurement noise and disturbance, the overall controlled system can be written in the following augmented form:

$$\dot{x}_a = A_a x_a + \bar{B}_a(r - y) + L_a w$$

$$y = C_a x_a + n \tag{3}$$

where

$$x_a = \begin{bmatrix} x_c \\ x_p \end{bmatrix}$$

and

$$A_a = \begin{bmatrix} 0 & 0 \\ B & A \end{bmatrix}, \quad \bar{B}_a = \begin{bmatrix} K_i \\ B & K_p \end{bmatrix}, \quad L_a = \begin{bmatrix} L_L \\ L_H \end{bmatrix}$$

$$C_a = [0 \quad C] \tag{4}$$

The dynamic driving noise w with distribution matrix L_a can be accounted for as modeling error with the assumption of Gaussian distribution, zero mean, and variance $\mathbf{W}$. Also, the measurement is assumed to be contaminated by Gaussian noise n with zero mean and
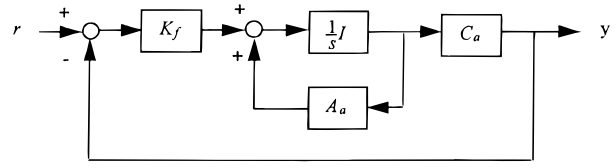

Figure 1. Target model with the Kalman filter loop.

variance $\mathbf{N}$. L_L and L_H are submatrices of L_a corresponding to the low- and high-frequency ranges, respectively. As a result, the PI-controlled system is essentially an output feedback control design that can be rewritten as follows:

$$\dot{x}_a = A_a x_a + \bar{B}_a u_a + L_a w$$

$$y = C_a x_a + n$$

$$u_a = K_a(r - y) \tag{5}$$

with

$$\bar{B}_a = B_a K_a, \quad B_a = \begin{bmatrix} I & 0 \\ 0 & B \end{bmatrix}, \quad K_a = \begin{bmatrix} K_i \\ K_p \end{bmatrix} \tag{6}$$

where the PI gain matrices are factored into K_a and u_a is a modified output feedback control signal. Since this augmented system equation shares the same design model $\{A_a, L_a, C_a\}$ used in the LQG/LTR loop shaping design (Athans, 1986), the LQG/LTR loop shaping design technique can be directly employed in the present robust PI controller design.

For many processes, the process model is frequently represented as a transfer matrix with time delays. We can use a rational approximation (e.g., the Padé approximation or all-pole approximation; Seborg et al., 1989) to obtain the state-space realization. A balanced state-space realization (Laub et al., 1987) is recommended to achieve a state-space model with equal controllability and observability properties.

3. Stage 1: Well-Decoupled Design through Model Matching

3.1. The Target Model. In general, stability and performance requirements can be conveniently represented in the frequency domain (Safonov et al., 1981; McFarlane and Glover, 1992). Information on parameter variations and unmodeled dynamics, such as neglected high-frequency modes or time delay, is summarized to form a high-frequency limit that is sufficient to specify the robust stability (Maciejowski, 1989). On the other hand, a low-frequency limit is specified to meet the requirements of tracking and disturbance rejection. In the loop shaping design technique, a desired loop transfer function which comprises all the performance specifications is assigned within the two limits mentioned above and serves as the target model. In the LQG/LTR loop shaping method, a target loop transfer matrix known as the Kalman filter loop (shown in Figure 1) is expressed as

$$G_{KF}(s) = C_a(sI - A_a)^{-1} K_f \tag{7}$$

where the matrix K_f is the Kalman filter gain (Athans, 1986). By selecting L_a, $\mathbf{W}$, and $\mathbf{N}$ as in eq 3 to assign a

desired loop shape of $G_{KF}(s)$, the K_f can be obtained by solving the well-known algebraic Riccati equation (ARE) as in the following:

$$P_f A_a^T + A_a P_f - P_f C_a^T N^{-1} C_a P_f + L_a \mathbf{W} L_a^T = 0$$

$$K_f = P_f C_a^T \mathbf{N}^{-1} \qquad (8)$$

Accordingly, the Kalman filter loop has the following guaranteed stability (Lehtomaki et al., 1981): (a) −6 dB to ∞ gain margin; (b) 60° phase margin. Moreover, the interactions in the multivariable system have been removed (Maciejowski, 1989). Interaction is undesirable as the ith output corresponding to the jth input. Therefore, the Kalman filter loop is suitable to serve as the target feedback loop in the present PI controller design.

As described in the appendix, the method of selecting L_a, $\mathbf{W}$, and $\mathbf{N}$ to obtain the desirable loop shape has been simplified to choosing a single design parameter, the crossover frequency ϖ_c, which is closely related to bandwidth and rise time. Guidelines for choosing ϖ_c to produce suitable loop shapes are also provided in the appendix.

3.2. PI Controller Approximation. By eq 5, the PI-controlled system has the following loop transfer function:

$$G_p(s) \, G_c(s) = C_a(sI - A_a)^{-1} B_a K_a \qquad (9)$$

where $G_p(s)$ and $G_c(s)$ are the transfer functions of the process and the PI controller, respectively. Equation 9 is similar to eq 7 for the Kalman filter loop except that K_f is replaced by $B_a K_a$. Their closed-loop system matrices are also represented similarly:

target model with Kalman filter loop

$$A_{c0} = A_a - K_f C_a = \begin{bmatrix} 0 & -K_{fL}C \\ B & A - K_{fH}C \end{bmatrix} \qquad (10)$$

PI-controlled system

$$A_c = A_a - B_a K_a C_a = \begin{bmatrix} 0 & K_i C \\ B & A - B K_p C \end{bmatrix} \qquad (11)$$

With suitable selection of the PI gain matrices K_a, the system matrix of the PI output feedback design ($A_a - B_a K_a C_a$) will approach the output injection ($A_a - K_f C_a$) in the LQG/LTR target loop. The model matching result is summarized in the following theorem:

Theorem 1. Let A_{c0} be the closed-loop system matrix of a target Kalman filter loop as described in eq 10, and let A_c be the closed-loop system matrix of the PI-controlled process as described in eq 11. The PI controller gain matrices as

$$K_i = K_{fL} \qquad (12)$$

$$K_p = (B^T \quad B)^{-1} B^T K_{fH} \qquad (13)$$

achieve the minimum norm solution, which minimizes the Frobenius norm of $||A_c - A_{c0}||_F$.

Proof. To minimize $||A_c - A_{c0}||_F$, with eqs 10 and 11, we have

$$||A_c - A_{c0}||_F^2 = ||B_a K_a C_a - K_f C_a||_F^2$$

$$= \text{trace}\{(B_a K_a C_a - K_f C_a)^T \times (B_a K_a C_a - K_f C_a)\}$$

If $||A_c - A_{c0}||_F^2$ is minimized with respect to $K_a C_a$, we obtain

$$K_a C_a = (B_a^T \quad B_a)^{-1} B_a^T K_f C_a$$

Furthermore, as long as C_a is of full rank, K_a is uniquely determined as in the following:

$$K_a = (B_a^T \quad B_a)^{-1} B_a^T K_f \qquad (14)$$

Full rank of C_a is essential for the system's observability requirement. Then, substitute the following matrices into eq 14:

$$K_a = \begin{bmatrix} K_i \\ K_p \end{bmatrix} \qquad B_a = \begin{bmatrix} I & 0 \\ 0 & B \end{bmatrix} \qquad \text{and} \qquad K_f = \begin{bmatrix} K_{fL} \\ K_{fH} \end{bmatrix}$$

We obtain the PI gain matrices

$$K_i = K_{fL}$$

$$K_p = (\mathbf{B}^T \quad \mathbf{B})^{-1} \mathbf{B}^T K_{fH} \qquad \square$$

3.3. Discussion. By Theorem 1, the PI-controlled system is matched to the target model of the Kalman filter loop to ensure its stability and well-decoupled output responses. Discussion of the first design stage is made as follows:

(1) If performance is satisfied in the first stage.

By eqs 12 and 13, we can see that, if each column of K_{fH} lies precisely in the subspace spanned by the columns of the **B** matrix, i.e.

$$K_{fH} \in \text{range}(\mathbf{B}) \qquad (15)$$

the PI-controlled loop will perfectly match the target Kalman filter loop. Satisfactory performance can thus also be guaranteed in the first design stage alone. Some well-known processes, such as stirred tanks (Kwakernaak and Sivan, 1972; Pulleston and Mantz, 1993), are particular cases.

In fact, the condition of eq (15) is very restrictive. Nevertheless, as will be shown in the first simulation example, although approximation error exists, satisfactory results can still be obtained in the first stage since both the closed-loop poles and the frequency loop shapes (singular value plots) are well-approximated for the PI-controlled system.

(2) If the interaction is significant.

By Theorem 1, its approximation error can be represented as

$$||\{\mathbf{B}(\mathbf{B}^T \quad \mathbf{B})^{-1} \mathbf{B}^T - \mathbf{I}\} K_{fH} C||_F \qquad (16)$$

Equation 16 indicates that the approximation error is system-dependent and affected by matrices **B** and **C**. However, we can reduce K_f to improve the model matching error; it can be accomplished by selecting a smaller ϖ_c (see eq A4 in the appendix) to obtain a smaller L_a and K_f (Willems, 1971). Consequently, interaction can be reduced.
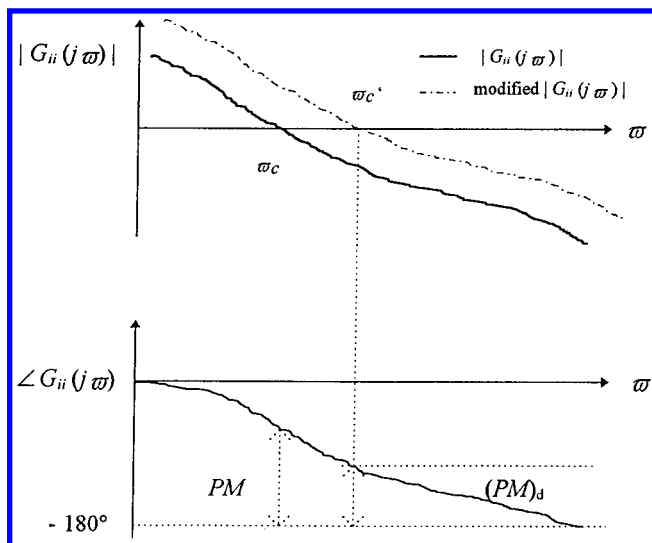
Figure 2. Strategy of PI gains modification in the proposed equivalent open-loop transfer function $G_{ii}(j\varpi)$. PM: phase margin. $(PM)_d$: desired phase margin.

(3) If the control performance is not satisfied.

Although we can obtain well-decoupled design in the first stage as above, the corresponding output responses may be sluggish or have undesirable overshoot. Therefore, we propose a second design stage to achieve a desirable performance without causing deterioration in terms of interaction.

4. Stage 2: Well-Damped Design by Modifying the Gain

Because a well-decoupled design can be achieved in the first stage, the multivariable control loop can be recognized as multiple independent loops. Thus, classical gain design can be employed to achieve desirable phase and gain margins. For the closed-loop transfer function $T_{ii}(s)$ from the setpoint r_i to the output y_i, an equivalent open-loop transfer function $G_{ii}(s)$ can be obtained as follows:

$$G_{ii}(s) = \frac{T_{ii}(s)}{1 - T_{ii}(s)} \tag{17}$$

Since the phase margin is closely related to the damping ratio of the dominant closed-loop poles, the controller gains can thus be adjusted to obtain a desirable phase margin of $G_{ii}(j\varpi)$, meeting a specified value corresponding to a desired damping behavior of the output responses.

Graphical interpretation of the proposed tuning strategy in the second stage is shown in Figure 2. If the phase margin of an initial design is not satisfied, we can determine the frequency ϖ_c' in the phase plot of $G_{ii}(j\varpi)$ with a desirable phase margin. Then, we can add suitable gain at this frequency point to 0 dB as the new crossover frequency. In this fashion, for an nth input/output system, a diagonal gain **K**

$$\mathbf{K} = \begin{bmatrix} \dfrac{1}{|G_{11}(j\varpi_{c1}')|} & & 0 \\ & \cdot & \\ & & \cdot \\ & & & \cdot \\ 0 & & \dfrac{1}{|G_{nn}(j\varpi_{cn}')|} \end{bmatrix} \tag{18}$$

is multiplied by the original PI controller $G_c(s)$ to obtain modified PI gains as

$$\tilde{G}_c(s) = G_c(s)\,\mathbf{K} = \frac{I}{s}K_i\mathbf{K} + K_p\mathbf{K} \tag{19}$$

Accordingly, the well-decoupled behavior is unchanged solely by postmultiplying a diagonal gain matrix **K** to $G_c(s)$. However, the frequency responses of the controlled process are improved to achieve well-damped output behavior with the specified phase margin.

Note that the tradeoff between the desired phase margin and the crossover frequency in the design implies the inherent limitation of the output feedback PI controller which is in a simple structure. In other words, if the response after stage 2 is not fast enough, another controller of higher order such as the LQG/LTR controller should be considered to further improve the design.

The proposed two-stage design procedure for the robust PI controller is summarized as below.

Design Procedure. Data: Given {**A**, **B**, **C**}.

Stage 1 (well-decoupled design)

Step 1. Set $\mathbf{W} = \mathbf{N} = \mathbf{I}$ (identity matrix) and determine L_a by selecting ϖ_c (eq A4).

Step 2. Obtain the Kalman filter gain K_f in eq 8.

Step 3. Obtain the PI gain matrices K_i and K_p by eqs 12 and 13.

If the performance of the design is not satisfied, continue the design into stage 2 for further damping improvement.

Stage 2 (well-damped design)

Step 1. Compute $T(s)$ of the initial design and obtain the corresponding $G_{ii}(s)$ by eq 17.

Step 2. From a Bode plot of each $G_{ii}(s)$, find the frequency ϖ_{ci}' and $|G_{ii}(j\varpi_{ci}')|$.

Step 3. Compute the diagonal gain **K** by eq 18 and the resulting PI controller in eq 19.

5. Examples

Example 1. A High-Purity Distillation Column. Consider the high-purity distillation column of Skogestad and Morari (1988). In this process, the top composition (y_D) and bottom composition (x_B) are controlled by manipulating the reflux (L) and boilup (V). For the case of negligible reboiler and condenser holdup, at specific nominal operating points of $y_D = 0.9$ and $x_B = 0.002$, a properly scaled two-time-constant model which yields a satisfactory approximation of the 41st-order linear model is as follows:

$$\begin{bmatrix} \Delta y_D/0.1 \\ \Delta x_B/0.002 \end{bmatrix} = G(s) \begin{bmatrix} \Delta L \\ \Delta V \end{bmatrix}$$

with

$$G(s) = \begin{bmatrix} \dfrac{16.0}{1 + T_1 s} & \dfrac{16.0}{1 + T_1 s} + \dfrac{0.023}{1 + T_2 s} \\ \dfrac{9.3}{1 + T_1 s} & \dfrac{-9.3}{1 + T_1 s} - \dfrac{1.41}{1 + T_2 s} \end{bmatrix}$$

where $T_1 = 24.5$ min and $T_2 = 10$ min and $\Delta(:)$ denotes the perturbation variable with respect to the nominal operating point. A balanced state-space realization of the above transfer matrix can be obtained as
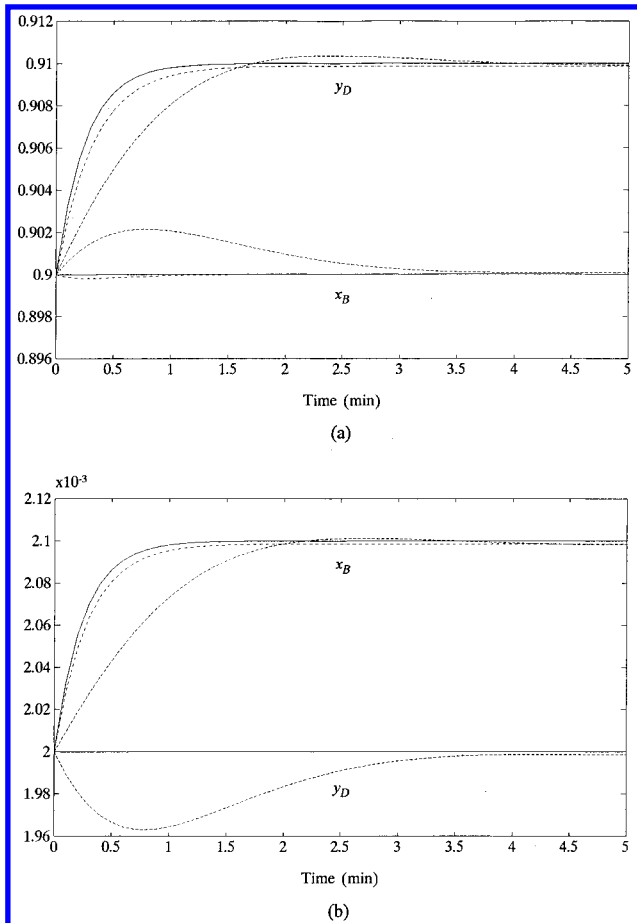
(a)

(b)

Figure 3. (a) Setpoint change in y_D and (b) small setpoint change in x_B for the PI controller (solid), multiloop PI controller of Skogestad and Morari, 1988 (dashed), and their PI controller with static decoupler (dash-dot).

$$\mathbf{A} = \begin{bmatrix} -0.0410 & 0.00002 & -0.0011 \\ 0.0029 & -0.0443 & 0.0167 \\ -0.0095 & 0.0115 & -0.0964 \end{bmatrix}$$

$$\mathbf{B} = \begin{bmatrix} 0.6542 & 0.7081 \\ 0.5532 & -0.5591 \\ 0.0027 & 0.1501 \end{bmatrix}$$

$$\mathbf{C} = \begin{bmatrix} 0.9605 & 0.0446 & 0.0010 \\ -0.0833 & 0.7853 & -0.1502 \end{bmatrix}$$

In the first-stage controller design, after referring to the rise time of the reported responses of Skogestad and Morari (1988), the crossover frequency was chosen as 5 rad/min for each loop. The proposed PI controller is obtained as

$$K_i = \begin{bmatrix} 0.1671 & 0.2501 \\ 0.1452 & -0.2497 \end{bmatrix} \qquad K_p = \begin{bmatrix} 4.3748 & 5.5162 \\ 3.2127 & -5.5451 \end{bmatrix}$$

The resulting PI-controlled system properly matches the target model in the Kalman filter loop, and they have very similar closed-loop poles as shown below.

closed-loop poles of the target model:

$$\{-0.0408, -0.0465, -0.0878, -5.0001 \pm 0.0003j\}$$

closed-loop poles of the present PI design:

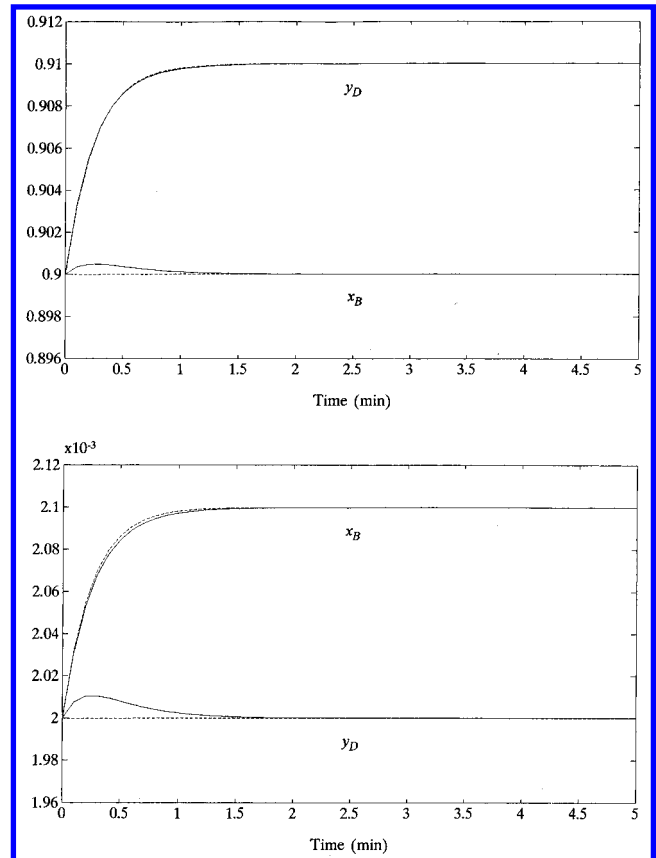$$\{-0.0414, -0.0451, -0.0905, -4.9299, -5.0002\}$$

Figure 4. Responses of the proposed PI design without input uncertainty (dashed) and with uncertainty (solid).

Moreover, their frequency loop shapes (singular value plots) are almost the same in all frequencies. The advantages of guaranteed stability and performance can be preserved for the present PI-controlled system.

Simulation results of the proposed PI controller were compared with the results obtained by Skogestad and Morari (1988). As shown in Figure 3, the proposed PI controller achieves fully decoupled and well-damped output response and renders better performance in all tracking accuracy and damping behavior.

To evaluate the proposed PI controller under modeling error, the following input uncertainties are included (Skogestad and Morari, 1988):

$$\Delta L = (1 + \Delta_1)\Delta L_c, \qquad \Delta_1 = 0.2$$

$$\Delta V = (1 + \Delta_2)\Delta V_c, \qquad \Delta_2 = -0.2$$

Here ΔL and ΔV are the actual changes in manipulated flow rates, while ΔL_c and ΔV_c are the desired values as computed by the controller. With the proposed PI design, a slight deterioration in time responses, as shown in Figure 4, indicates that the proposed PI design is robust with regard to the discussed uncertainties.

Example 2. A Chemical Process That Produces a Solution of Ammonia and Urea. Consider the chemical process discussed in Lunze (1989). The output variables of the process are the concentrations of ammonia (C_A) and urea (C_U) within the final solution; these should be maintained at a constant level during operation. The input variables are the quantity of the second component flowing through an input valve and the temperature of the initial solution. The coefficient matrices of its state-space representation are as follows:
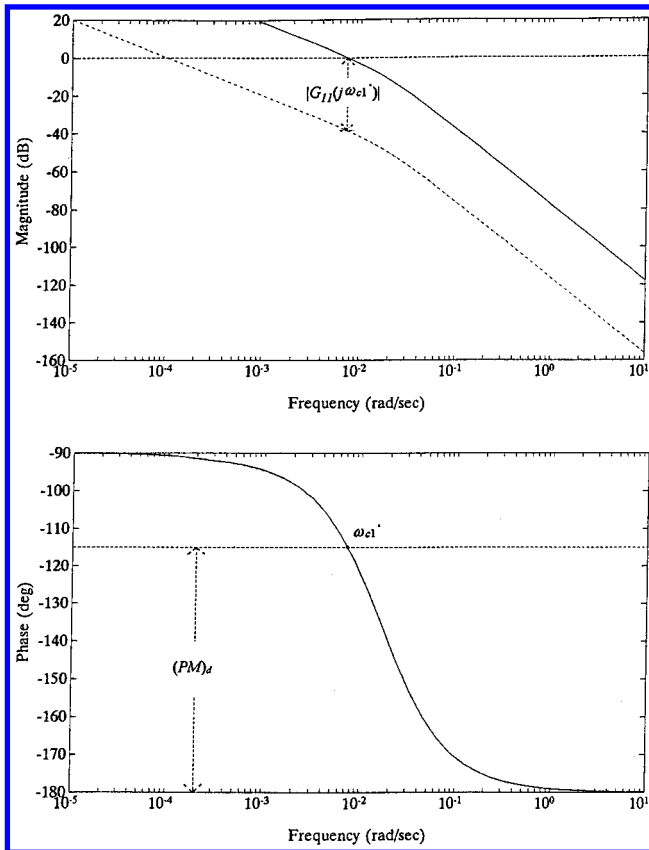
$$A = \begin{bmatrix} -0.00606 & 0 & & & & & & & 0 \\ 0.00166 & -0.00166 & & & & & & & \\ & & -0.00641 & 0 & & & & & \\ & & 0.00084 & -0.00084 & & & & & \\ & & & & -0.00641 & 0 & & & \\ & & & & 0.00166 & -0.00166 & & & \\ & & & & & & -0.00084 & 0 & \\ & & 0 & & & & 0.00040 & -0.00040 \end{bmatrix}$$

$$B = \begin{bmatrix} 0.00606 & 0 \\ 0 & 0 \\ 0 & 0.00641 \\ 0 & 0 \\ 0.00641 & 0 \\ 0 & 0 \\ 0 & 0.00084 \\ 0 & 0 \end{bmatrix} \qquad C = \begin{bmatrix} 0 & 2.2 & 0 & 0.033 & 0 & 0 & 0 & 0 \\ 0 & 0 & 0 & 0 & 0 & -0.026 & 0 & 0.09 \end{bmatrix}$$

Stage 1 (Well-Decoupled Design). Referring to the rise time of the reported responses of this chemical process (approximately 194 min, as shown in Lunze, 1989), the crossover frequency can be set as 0.0001 rad/s (Franklin et al., 1994). Following the design procedure we have described, we obtain an initial design with the following PI gain matrices:

$$K_i = \begin{bmatrix} 4.4077 \times 10^{-6} & -1.1097 \times 10^{-5} \\ 1.2270 \times 10^{-4} & 1.0828 \times 10^{-3} \end{bmatrix}$$

$$K_p = \begin{bmatrix} 0.0069 & -0.0025 \\ 0.0215 & 0.1815 \end{bmatrix}$$

The closed-loop poles of the target model and the PI-controlled system are similar:

closed-loop poles of the target model:

$$\{-0.0001, -0.0001, -0.0004, -0.0008, -0.0008, \\ -0.0061, -0.0064 \pm 5 \times 10^{-6}j, -0.0166\}$$

closed-loop poles of the present PI design:

$$\{-0.0001, -0.0002 \pm 0.0001j, -0.0008, -0.0009, \\ -0.0061, -0.0064 \pm 2 \times 10^{-6}j, -0.0165\}$$

The corresponding singular value plots of the PI-controlled loop and the Kalman filter loop, as shown in Figure 5, indicate that they are different in the high-frequency range. Consequently, the phase characteristics of the PI-controlled system deviate from the target model in the high-frequency region. Although a well-decoupled design is accomplished in the first stage, response is sluggish because of choosing a small crossover frequency. Therefore, the PI controller requires further modification to achieve a desirable phase margin.

Stage 2 (Well-Damped Design). Frequency responses of the first-stage design are as shown in Figurea 6 and 7 for loops 1 and 2, respectively. If the desired phase margins are selected as 65° for loop 1 and 60° for loop 2, following the proposed algorithm the gain **K** can be obtained as

$$K = \begin{bmatrix} 83.9441 & 0 \\ 0 & 1.7547 \end{bmatrix}$$

Figure 5. Singular value plots of the Kalman filter loop (dashed) and the PI-controlled loop (solid).

The final controller gains are then obtained:

$$K_i = \begin{bmatrix} 0.0037 & -0.00003 \\ 0.0103 & 0.0019 \end{bmatrix} \qquad K_p = \begin{bmatrix} 0.5806 & -0.0044 \\ 1.8016 & 0.3184 \end{bmatrix}$$

The phase margin of each loop can then be adjusted satisfactorily:

loop 1 (concentration of ammonia)

crossover frequency, 0.00720 rad/s;
phase margin, 65.04°

loop 2 (concentration of urea)

crossover frequency, 0.00016 rad/s;
phase margin, 59.99°

As shown in Figure 8, a well-decoupled design is obtained in the first stage but with sluggish response, while the rise time of the responses have been significantly improved in the second stage to achieve both well-decoupled and well-damped performance.

Compare this with the results reported in Lunze (1989). As shown in Figure 9a, the present PI design achieves the best results in the responses to a unit step change in C_A. In the time responses to a unit step change in C_U as shown in Figure 9b, Lunze's result exhibits a quicker response but with larger interaction. In summary, the proposed PI controller achieves a

Figure 6. Bode plots of the equivalent open-loop transfer function $G_{11}(j\varpi)$ for stage 1 (dashed) and stage 2 (solid). (PM)$_d$: desired phase margin.
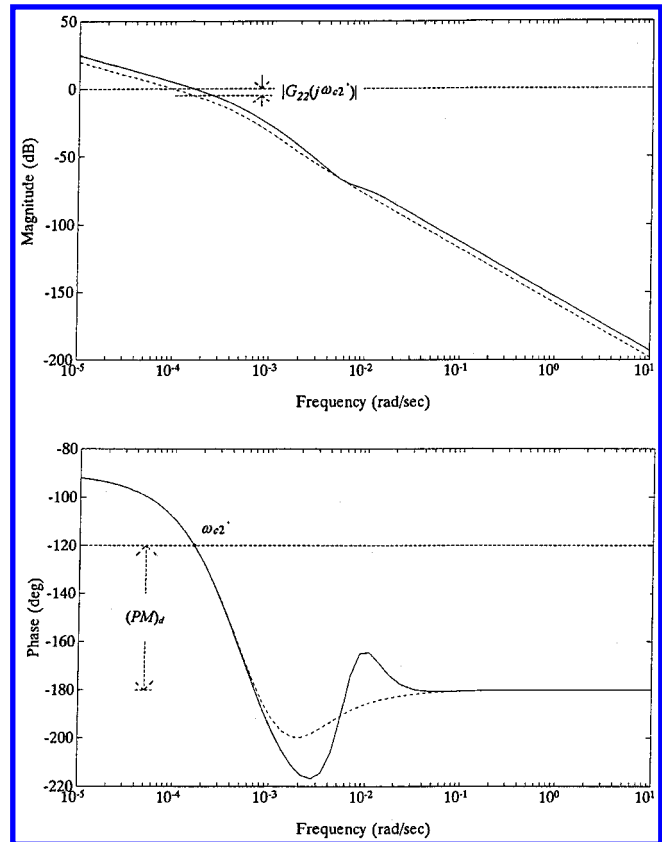

Figure 7. Bode plots of the equivalent open-loop transfer function $G_{22}(j\varpi)$ for stage 1 (dashed) and stage 2 (solid). (PM)$_d$: desired phase margin.

better overall control performance. Note that we directly achieve the present PI controller, while in Lunze's design the controller was fine-tuned by trial-and-error.

Example 3. Application to a Supersonic Wind Tunnel Experiment. The high-speed wind tunnel systems are commonly used to test the performance of high-speed flight vehicles under various conditions (Pope and Goin, 1965; Soeterboek et al., 1991; Hwang and Hsu, 1992). With a chosen nozzle and the referred Standard Atmosphere Table (NOAA, 1976), the experimental conditions of Mach number and altitude can be transformed into the conditions of the setting pressure and temperature in the wind tunnel system. They are achieved via proper operations of the air and fuel control valves (refer to Figure 10). Based on the mass and energy balance principles, nonlinear governing equations for the present supersonic wind tunnel system were derived by Hwang and Hsu (1992) and Hwang (1997). A properly scaled linearized nominal model of the wind tunnel is

$$
\mathbf{A} = \begin{bmatrix} -21.0 & -0.3 & 0 & 0 \\ -140.8 & -15.7 & 0 & 0 \\ 2.6 & 0 & -21.5 & -0.1 \\ -281.7 & 25.2 & -1556.8 & -16.6 \end{bmatrix}
$$

$$
\mathbf{B} = \begin{bmatrix} 7.1 & 0 \\ 57.2 & 0 \\ 0 & 1.5 \\ 0 & 310.4 \end{bmatrix} \qquad \mathbf{C} = \begin{bmatrix} 1/10.36 & 0 & 0 & 0 \\ 0 & & 0 & 0 & 1/623 \end{bmatrix}
$$

The state x and input u are

$$
x(t) = \begin{bmatrix} P_1(t) - P_{10} \\ T_1(t) - T_{10} \\ P_2(t) - P_{20} \\ T_2(t) - T_{20} \end{bmatrix} \quad u(t - T_d) = \begin{bmatrix} u_a(t - T_{da}) - u_{a0} \\ u_f(t - T_{df}) - u_{f0} \end{bmatrix}
$$

P_1 = pressure in plenum 1 (bar), T_1 = temperature in plenum 1 (K), P_2 = pressure in plenum 2 (bar), T_2 = temperature in plenum 2 (K), u_a = air control valve opening ($0-100$), and u_f = fuel control valve opening ($0-100$). Based on the testing flight conditions of the Mach number 3.3 and the altitude 19.82 km, the corresponding operating conditions are as in the following (Hwang, 1997): $P_{10} = 10.36$ bar, $T_{10} = 298$ K, $P_{20} = 3.25$ bar, $T_{20} = 623$ K, $u_{a0} = 32.5$ opening, and $u_{f0} = 32.5$ opening. The tracking variables are P_1 and T_2, and they are normalized by the nominal operating points, as shown in the output matrix **C**. The distributed characteristics of the process and the time lag involved in the combustion process are summarized as input delays T_{da} and T_{df} for pressure and temperature control, respectively, with

$$
T_{da} \approx 0.8 \text{ s}, \qquad T_{df} \approx 2.0 \text{ s}
$$

To this time-delayed process, the delay-free nominal model as described is employed for the controller design. The time delay effect is considered as the modeling error. As computed from the model difference between the time-delayed model and the delay-free model, the corresponding uncertainty profile (Maciejowski, 1989) shown in Figure 11 indicates that the crossover frequency should be chosen within 0.5 rad/s to satisfy the
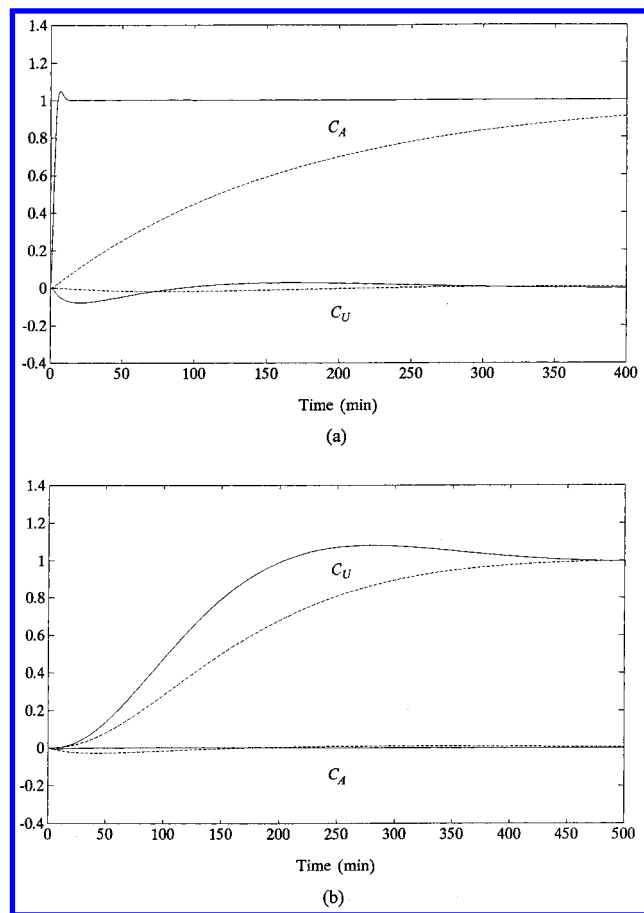
Figure 8. Results of stage 1 (dashed) and stage 2 (solid) subjected to (a) unit step change in C_A and (b) unit step change in C_U.

Figure 9. Results of example 2 (a) unit step change in C_A and (b) unit step change in C_U for the present PI controller (solid) and the PI controller of Lunze, 1989 (dash-dot).

robust stability. Following the proposed two-stage design procedure with desirable phase margins of 70° for pressure control and 65° for temperature control, the resulting controller gain matrices are obtained as

$$K_i = \begin{bmatrix} 13.2687 & 0.0657 \\ 8.9654 & 8.3538 \end{bmatrix} \qquad K_p = \begin{bmatrix} 0.1684 & 0.0005 \\ 0.0042 & 0.4229 \end{bmatrix}$$

In the present experiments, the desired pressure P_1 and temperature T_2 in the closed-loop control are set as 10.36 bar and 350 °C, respectively (Hwang, 1997). Figure 12 shows that the present PI controller achieves well-damped behavior in both pressure and temperature responses in the initial test with the cold wind tunnel. To verify the achieved control performance under different operating conditions, the setpoint of P_1 is changed from 10.36 to 11.72 bar. As shown in Figure 13, more significant interaction exists between P_1 and T_2 due to the model inaccuracy with the heated wind tunnel after repeated tests. The responses were still acceptable from the practical point of view. Moreover, the nonlinear and time-varying characteristics of the process can be observed by comparing the temperature responses as shown in Figures 12 and 13. Figure 13 of an another test shows more damped behavior. The existing non-linearity and uncertainty limit the selection of higher crossover frequencies that may speed up the responses, because large overshoot may be induced which increases the risk of combustion instability, especially to the wind tunnel. Overall, the present robust PI controller design achieves both satisfactory stability and control performance.
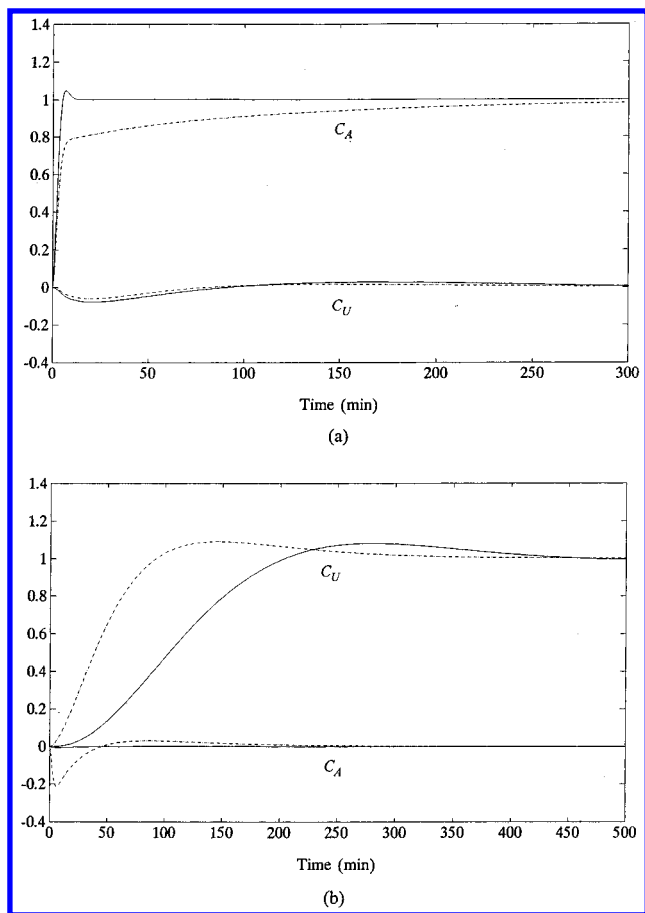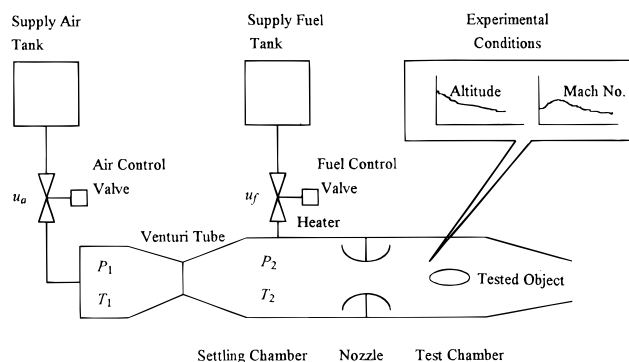

Figure 10. Schematic diagram of a supersonic intermittent blowdown wind tunnel.

6. Conclusions

In this paper, we have proposed a systematic design procedure to obtain robust PI controllers for multivariable processes. The following points can be concluded concerning the proposed two-stage design procedures:

(1) With suitable formulation, the PI-controlled loop can be very similar to the Kalman filter loop in the LQG/LTR approach. The PI-controlled loop can be thus easily matched to the target Kalman filter loop in the first stage via the model matching theorem we have developed.

(2) Well-decoupled design can usually be achieved in the first stage by choosing a smaller crossover frequency. Moreover, the robustness issues in the LQG/LTR approach can be directly applied to the design of the robust PI controller.
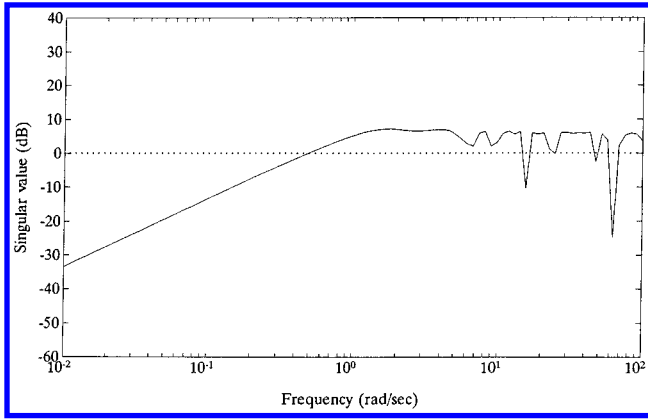
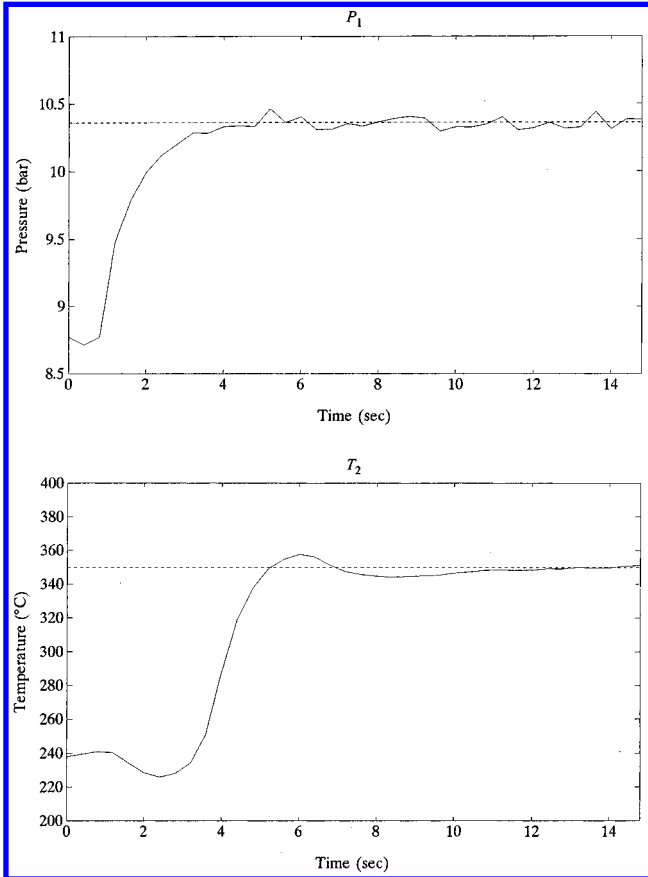**Figure 11.** Uncertainty profile of the wind tunnel model.

Figure 12. Experimental results with a cold wind tunnel.

(3) Due to the existing approximation error, if the performance in the first stage design is not satisfactory, it can be effectively improved by applying classical gain modification as proposed in the second stage. Because of the limitations of the PI controller, if response after the second-stage design is not fast enough, another controller of higher order, such as the LQG/LTR controller, should be considered to improve the design.

The results of the two simulation examples and the supersonic wind tunnel experiment show that the present PI controller achieves well-decoupled and well-damped output behavior. The proposed two-stage design, providing straightforward procedures and guaranteed performance, should be very useful in real industrial applications.

Appendix: Method of Selecting L_a, W, and N

In the LQG/LTR loop shaping design technique, the desired loop shape of the Kalman filter loop is assigned
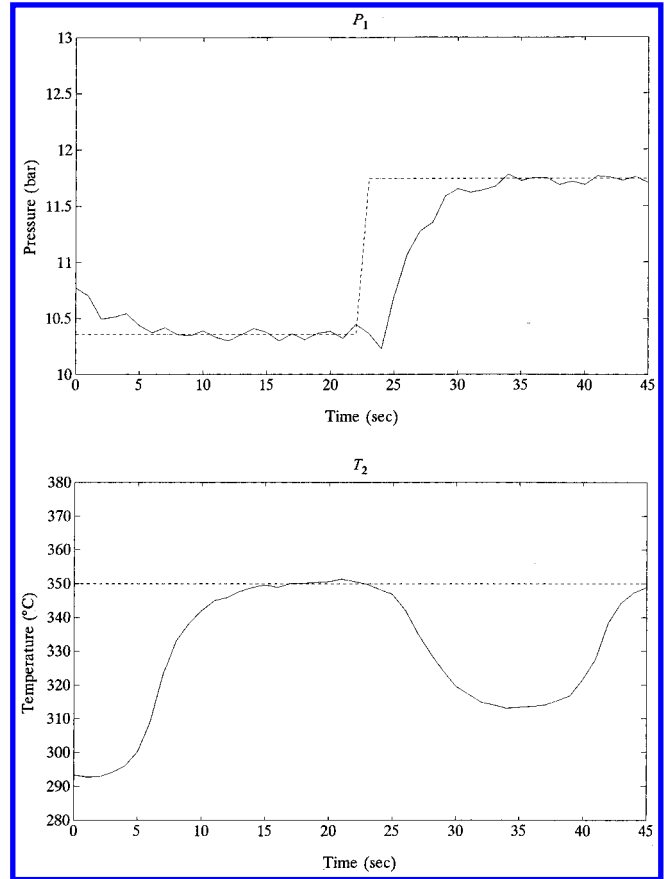

Figure 13. Experimental results with a heated wind tunnel.

by selecting appropriate L_a, **W**, and **N**. Theoretically, when the smallest singular values of the Kalman filter loop $\sigma[G_{KF}] \gg 1$, the Kalman equality shows that (Stein and Āthans, 1987)

$$\sigma_i[C_a(j\omega I - A_a)^{-1}K_f] \approx \sigma_i[C_a(j\omega I - A_a)^{-1}L_a W^{1/2}] \quad \text{(A1)}$$

where $\sigma_i[:]$ represents the ith singular value of the discussed transfer matrix, and the $\mathbf{W}^{1/2}$ in the equation represents the square root decomposition of matrix **W** and

$$\mathbf{W} = \mathbf{W}^{1/2}(\mathbf{W}^{1/2})^{\mathrm{T}}$$

Thus, the design parameters of matrices L_a and **W** can be adjusted to achieve the desired loop shape.

The Kalman filter loop of eq (7) has the following frequency properties (Stein and Athans, 1987):

$$\lim_{\omega \to 0} \sigma_i[C_a(j\omega I - A_a)^{-1}K_f] \approx \frac{I}{\omega}[\mathbf{C}(-\mathbf{A})^{-1}\mathbf{B}]K_{fL} \quad \text{(A2)}$$

$$\lim_{\omega \to \infty} \sigma_i[C_a(j\omega I - A_a)^{-1}K_f] \approx \frac{I}{\omega}\mathbf{C}K_{fH} \quad \text{(A3)}$$

and

$$K_f = \begin{bmatrix} K_{fL} \\ K_{fH} \end{bmatrix}$$

If the open-loop system matrix **A** is invertible, a popular target loop transfer function can be adopted where the singular values of the loop are matched at both low and high frequencies (Ridely, 1987; Garg, 1989). To achieve a matched Kalman filter loop shape, we can simply set $\mathbf{W} = \mathbf{N} = \mathbf{I}$ (identity matrix) in eq 8

and choose L_L and L_H of L_a as

$$L_L = [\mathbf{C}(-\mathbf{A})^{-1}\mathbf{B}]^{-1}\varpi_c$$

$$L_H = C^T \,(\mathbf{C} \quad \mathbf{C}^T)^{-1}\varpi_c \tag{A4}$$

where ϖ_c is the assigned crossover frequency. As a result, the singular values of the Kalman filter loop can approach $(\mathbf{I}/\varpi)\varpi_c$ in both the low- and high-frequency regions. Then, K_f can be obtained by eq 8.

It should be noted here that K_f obtained from the selection of L_a in eq A4 may tend to "invert the plant"; i.e. the closed-loop poles will be very close to the stable images of the open-loop poles, as noted by Ridely (1987). Therefore, if the open-loop system contains lightly damped poles, the selection of eq A4 may result in oscillatory time responses; i.e., the loop characteristics in the mid-frequency range may not be satisfactory. Under such circumstances, another loop function (e.g., Maciejowski, 1989) is preferred.

Guideline for Choosing ϖ_c. As shown in eq A4, ϖ_c is the major design parameter for adjusting the Kalman filter loop shape. The achievable ϖ_c should not be beyond the high-frequency limit observed from the uncertainty profile (Ridely, 1987; Maciejowski, 1989) in order to achieve robust stability. It should also take into account the physical limit inherent in the actuator. On the other hand, because ϖ_c is closely related to the reaction speed, e.g., for a system with second-ordered dominant poles, the rise time t_r and the ϖ_c for a damping ratio of 0.7 can be represented as (Franklin et al., 1994)

$$t_r \approx 1.165/\varpi_c$$

A lower bound of ϖ_c can thus be specified as the lowest limit of the required speed of responses.

Literature Cited

Åström, K. J.; Hägglund, Y.; Hang, C. C.; Ho, W. K. Automatic Tuning and Adaptation for PID Controllers—a Survey. *Control Eng. Pract.* **1993**, *1*, 699–714.

Athans, M. A Tutorial on The LQG/LTR Method. Proceedings of the American Control Conference, Seattle, WA, 1986; pp 1289–1296.

Bristol, E. H. On a New Measure of Interaction for Multivariable Process Control. *IEEE Trans. Autom. Control* **1966**, *11*, 133–134.

Chen, C. L.; Munro, N. Procedure to Achieve Diagonal Dominance Using a PI/PID Controller Structure. *Int. J. Control* **1989**, *50*, 1771–1792.

Deshpande, P. B. *Multivariable Process Control*; Institute Society of America: Research Triangle Park, NC, 1989.

Franklin, G. F.; Powell, J. D.; Abbas, E. N. *Feedback Control of Dynamic Systems*; Addison-Wesley, Reading, MA, 1994.

Friman, M.; Waller, K. V. Autotuning of Multiloop Control System. *Ind. Eng. Chem. Res.* **1994**, *33*, 1708–1717.

Garg, S. Turbofan Engine Control System Design Using the LQG/LTR Methodology. In Proceedings of American Control Conference, Pittsburgh, PA, 1989; pp 134–141.

Grosdidier, P.; Morari, M. Interaction Measures for Systems under Decentralized Control *Automatica* **1986**, *22*, 309–319.

Han, Z. Z. Eigenstructure Assignment Using Dynamical Compensator. *Int. J. Control*, **1989**, *49*, 233–245.

Hwang, S. H. Geometric Interpretation and Measures of Dynamic Interactions in Multivariable Control Systems. *Ind. Eng. Chem. Res.* **1995**, *34*, 225–236.

Hwang, D. S. Robust Control and Diagnostic System Design for the Supersonic Wind Tunnel. Ph.D. Dissertation, National Chiao-Tung University, Hsinchu, Taiwan, 1997.

Hwang, D. S.; Hsu, P. L. The LQG/LTR Controller Design for the Wind Tunnel. Proceedings of 11th IASTED Conference on Modeling, Identification and Control, Innsbruck, 1992; pp 371–374.

Knoop, M. K. F.; Perez, J. A. M. Approximate Model matching with Multivariable PI-Controller. *Automatica* **1993**, *29*, 1615–1616.

Kwakernaak, H.; Sivan, R. *Linear Optimal Control Systems*; John Wiley & Sons: New York, 1972.

Laub, A. J.; Heath, M. T.; Paige, C. C.; Ward, R. C. Computation of System Balancing Transformations and Other Applications of Simultaneous Diagonalization Algorithms. *IEEE Trans. Autom. Control* **1987**, *32*, 115–122.

Lehtomaki, N. A.; Sandell, N. R.; Athans, M. Robustness Results in Linear Quadratic Gaussian Based Multivariable Control Design. *IEEE Trans. Autom. Control* **1981**, *26*, 75–92.

Lewis, F. L. *Applied Optimal Control and Estimation*; Prentice-Hall International: Englewood Cliffs, NJ, 1992.

Loh, A. P.; Hang, C. C.; Quek, C. K.; Vasnani, V. U. Autotuning of Multiloop Proportional–Integral Controllers Using Relay Feedback. *Ind. Eng. Chem. Res.* **1993**, *32*, 1102–1117.

Lunze, J. *Robust Multivariable Feedback Control*; Prentice-Hall International: Englewood Cliffs, NJ, 1989.

Luyben, W. L. Simple Method for Tuning SISO Controllers in Multivariable Systems. *Ind. Eng. Chem. Process Des. Dev.* **1986**, *25*, 654–660.

Maciejowski, J. M. *Multivariable Feedback Design*; Addison-Wesley: Reading, MA, 1989.

McFarlane, D.; Glover, K. A Loop Shaping Design Procedure Using H_∞ Synthesis. *IEEE Trans. Autom. Control* **1992**, *37*, 759–769.

Morari, M. Robust Stability of Systems with Integral Control. *IEEE Trans. Autom. Control* **1985**, *30*, 574–577.

NOAA, NASA, and USUF. *U. S. Standard Atmosphere*; U.S. Goverment Printing Office: Washington, DC, 1976.

Penttinen, J.; Koivo, H. N. Multivariable Tuning Regulators for Unknown Systems. *Automatica* **1980**, *16*, 393–398.

Pohjolainen, S. A. Robust Multivariable PI-controller for Infinite Dimensional Systems. *IEEE Trans. Autom. Control* **1982**, *27*, 17–30.

Pope, A.; Goin, K. L. *High Speed Wind Tunnel Testing*; John Wiley & Sons: New York, 1965.

Pulleston, P. F.; Mantz, R. J. Proportional Plus Integral MIMO Controller for Regulation and Tracking with Anti-Windup Feature. *Ind. Eng. Chem. Res.* **1993**, *32*, 2647–2652.

Ridely, D. B. Linear Quadratic Gaussian with Loop Transfer Recovery Methodology for An Unmanned Aircraft. *J. Guidance* **1987**, *10*, 82–89.

Safonov, M.; Hartmann G.; Laub, A. Feedback Properties of Multivariable Systems: The Role and Use of the Return Difference Matrix. *IEEE Trans. Autom. Control* **1981**, *21*, 47–63.

Seborg, D. E.; Edgar, T. F.; Mellichamp, D. A. *Process Dynamics and Control*; John Wiley and Sons: New York, 1989.

Skogestad, S.; Morari, M. LV-Control of a High-Purity Distillation Column. *Chem. Eng. Sci.* **1988**, *43*, 33–48.

Soeterboek, A. R. M.; Pels, A. F.; Verbruggen, H. B.; Van Largen, G. C. A. A Predictive Controller for the Mach Number in a Transonic Wind Tunnel. *IEEE Control Syst. Mag.* **1991**, Jan, 63–72.

Stein, G.; Athans, M. The LQG/LTR Procedure for Multivariable Feedback Control Design. *IEEE Trans. Autom. Control* **1987**, *32*, 105–114.

Willems, J. C. Least Squares Stationary Optimal Control and the Algebraic Riccati Equation. *IEEE Trans. Autom. Control* **1971**, *16*, 621–634.

Wong, K. P.; Seborg, D. E. Optimal Proportional Plus Integral Control for Regulator and Tracking Problems. *Optim. Control Appl. Methods* **1985**, *6*, 335–350.